International Journal of Automotive Technology, Vol. 1, No. 2, pp. 71–77 (2000)

1229–9138/2000/002–02

CREEP-FATIGUE CRACK GROWTH AND CREEP RUPTURE BEHAVIOR IN TYPE 316 STAINLESS STEELS − EFFECT OF HOLD TIME AND AGING TREATMENT

J. W. IM, S. J. WON, M. J. KIM and B. S. LIM*

School of Mechanical Engineering, Sungkyunkwan University, Suwon 440-746, Korea

(*Received 28 August 2000*)

ABSTRACT–High temperature materials in service are subjected to mechanical damage due to operating load and metallurgical damage due to operating temperature. Therefore, when designing or assessing life of high temperature components, both factors must be considered. In this paper, the effect of tensile hold time on high temperature fatigue crack growth and long term prior thermal aging heat treatment on creep rupture behavior were investigated using STS 316L and STS 316 austenitic stainless steels, which are widely used for high temperature components like in automotive exhaust and piping systems. In high temperature fatigue crack growth tests using STS 316L, as tensile hold time increased, crack growth rate decreased in relatively short tensile hold time region. In creep rupture tests with STS 316, as aging time increased, the values of creep stress exponent decreased. In long term aged specimens, cavity type microcracks have been observed at the interface of grain boundary and coarsened carbide.

KEY WORDS : High temperature fatigue crack growth, Hold time, Thermal aging, Creep-rupture

1. INTRODUCTION

Stainless steel has good high temperature strength and corrosion resistivity. Thus, it is used for exhaust system, mold, and muffler in automobile. Especially, austenitic stainless steel has outstanding machinability, weldability, and high temperature strength, which explains why it is being used for high operating temperature equipment such as pipe and tube in power plants besides automobile (Kim *et al*., 1996).

High temperature components are subjected to two types of damages during service. One is a mechanical damage caused by operating load and the other is a metallurgical damage caused by operating temperature.

Many structures or components are generally used under either static or cyclic load based on their operating conditions, but with some degree of differences, they are exposed to the operating conditions where both static and cyclic loads apply. When static load and cyclic load are applied simultaneously or repeatedly at high temperature, damage on a material due to creep deformation and crack nucleation and propagation due to fatigue cause an early fracture of components (Lee, 1997; Nam and Hong, 1984). Most materials show decrease in fatigue life as tensile hold time increases, but in some materials, fatigue life tends to increase when tensile hold time is relatively short (Parida and Nicholas, 1992; Adefris *et al*., 1996; Jata *et al*., 1994).

Generally, metallic materials creep at a homologous temperature greater than 0.4. A number of equipment that operate in power plants, petrochemical plants, oil refineries and airplanes are exposed to the creeping temperature. At creep condition, because of high temperature, microstructures of the structural alloys change continuously, and this change influences the creep properties.

Many studies have been reported on the effect of microstructures on creep and stress rupture behavior, which is associated with the grain size (Hong and Yu, 1989; Nakanishi, 1997) and the precipitates (Choe *et al.*, 1997). Particularly, studies, which are associated with the precipitation behavior, are consisted of matching fracture types to precipitates by long term creep rupture tests (Shinya *et al*., 1983; Biss, 1981; Shinya, 1985) and investigating the effects of precipitates on creep behaviors by prior aging treatment (Kim *et al.*, 1990). However, studies by the long term creep rupture tests are localized on the fracture surface, and most studies by prior aging treatments are of short term, and therefore, they do not reflect the precipitation behavior of the equipment served for long period at high temperature sufficiently. Therefore, to assess life of high temperature components, both mechanical and metallurgical damages

**Corresponding author.* e-mail:

must be considered.

In this study, high temperature fatigue crack behavior of STS 316L with various tensile hold times was examined and their effect on high temperature fatigue was analyzed using fracture mechanics parameter ΔK, and the effect of long term prior aging treatment on creep behavior in STS 316 was investigated also.

2. EXPERIMENTAL PROCEDURES

Table 1 shows the chemical composition of the STS 316L (AISI 316L) and the STS 316 (AISI 316) used for the test specimens.

All specimens were solutionized at 1130°C for 20 minutes in order to resolve precipitates which may exist in the matrix of austenite, and subsequently, they were water quenched to avoid the carbide precipitation at the grain boundaries during the cooling process. After the solution treatment, STS 316 was aged for different times of 0, 100, 1000 and 220 hr. at 750°C. The aging temperature was determined with the TTP (Time-Temperature-Precipitation) diagram of type 316 stainless steel (Shinya *et al*., 1982). According to the diagram, the typical precipitates that develop during the service, form fastest at 750°C. After the aging treatment, room temperature and high temperature tensile tests were carried out. Tensile test specimens were prepared according to KS B 0801 (1991). Room temperature tests were performed according to ASTM E 8 (1995) and high temperature tests at 650°C according to ASTM E 21 (1995).

To evaluate the effect of tensile hold time on high temperature fatigue crack growth of STS 316L, tensile hold time applied fatigue tests were carried out using solution treated specimens. Fatigue tests were carried out using a 10 ton capacity Shimadzu Dynamic Testing System at 600°C according to ASTM E 647 (1995). The test conditions are shown in Table 2. The short loading and unloading times, which were 0.05 sec each, were chosen to avoid creep effect during the loading and unloading. Figure 1 shows the geometry of the fatigue test specimen. Crack length was measured using Direct Current Potential Drop (DCPD) method.

To investigate the effect of thermal aging treatment on creep rupture behavior of STS 316, creep rupture tests were conducted with a 3 ton capacity dead weight type constant load creep machine (Shinwon SW-CFT3) according to ASTM E139 (1995). Figure 2 shows the geometry of the creep rupture specimen. The initial applied stresses for the aged specimens were ranged from 210 to 270 MPa and displacement was measured using LVDT (Kyowa DT-50A) system and the signal was amplified with signal conditioner (Instech SM-10) and recorded on PC. The strain was calculated according to ASTM E139.

To observe the precipitates formed after the aging treatment, an optical microscope was used and the grain size was measured to investigate the effect of the aging. To examine the microstructure, Gryceregia was used as

Table 1. Chemical composition (wt%).

Material	C	Si	Mn	P	S
316L	0.02	0.62	0.69	0.021	0.002
316	0.046	0.58	1.04	0.020	0.005
Material	Cr	Ni	Mo	Fe	
316L	17.37	12.23	2.16	Bal.	
316	16.29	10.55	2.10	Bal.	

Table 2. Conditions of the fatigue tests loading.

Hold time	Loading* waveform	Initial $\cdot K$ (MPa $\sqrt{m}$)	Final $\cdot K$ (MPa $\sqrt{m}$)
0 sec.	Triangular	15.4	23.6
5 sec.	Trapezoidal	15.1	25.3
10 sec.	Trapezoidal	14.6	25.3
50 sec.	Trapezoidal	20.6	26.6
100 sec.	Trapezoidal	20.4	26.4

*Loading (unloading) time is 0.05 sec and load ratio is 0.1

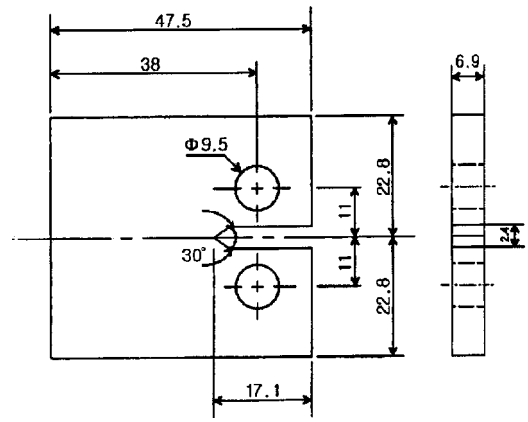

Figure 1. Geometry of fatigue crack growth test specimen.

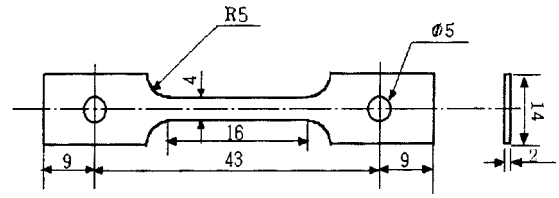

Figure 2. Geometry of creep rupture specimen.

an etchant to etch precipitates selectively.

To study the change of crack growth rate by fractography, aspects of the fracture surface due to tensile hold time were examined with Scanning Electron Microscope (SEM).

3. RESULTS AND DISCUSSION

3.1. Fatigue Crack Growth Rate Tests With Tensile Hold Time

Figure 3 shows the fatigue test results of 0 sec., 5 sec., 10 sec., 50 sec., and 100 sec. tensile hold time specimens with a *da*/*dN* and ΔK curve. The results of fatigue test with 0 sec. and 5 sec. tensile hold time were similar to each other as can be observed in the figure but the 5 sec. tensile hold time showed decrease in crack growth rate. Also, the crack growth rate for tensile hold time of 10 sec. decreased compared to the 0 sec. and 5 sec. ones. When the crack growth rates were compared within the ΔK range of 20.4 MPa$\sqrt{m}$ to 26.6 MPa$\sqrt{m}$, it can be seen that as the hold time increased from 0 to 10 sec., the rate decreased, however as hold times increased further to 50 and 100 sec., the rate ceased to decrease, but began to increase. When the pure fatigue crack growth rates and the tensile hold time applied fatigue crack growth rates were compared where ΔK is 23 MPa$\sqrt{m}$, the percent decreases were 10.5% for 5 sec., 40.5% for 10 sec., 42.0% for 50 sec., and 22.8% for 100 sec..

From the above results, it can be seen that within the ΔK range of this study, the STS 316L steel tends to decrease in crack growth rate compared to the pure fatigue one in the relatively short tensile hold time range.

To find the reason for decrease in the crack growth rate, another experiment was done as shown in Figure 4. Hold time of 80 min. is applied at three different crack lengths during the pure fatigue test and the decreasing behaviors of crack growth rate after application of the hold times were observed as shown in Figure 4. Based on the result, it can be concluded that tensile hold time

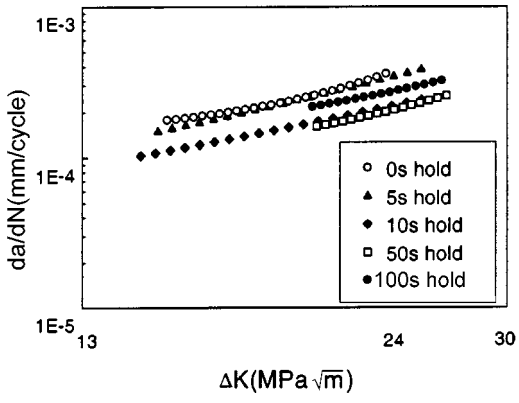

Figure 3. *da*/*dN* vs. ΔK curve at various tensile hold times (0, 5, 10, 50, and 100 sec.).

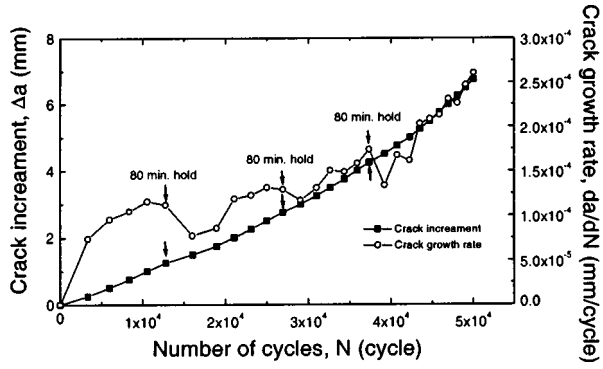

Figure 4. Results of a-N curve (solid square, ■) and the fatigue crack growth rate (open circle, ○) with hold times of 80 min. applied at the maximum load at different crack length at 600°C.

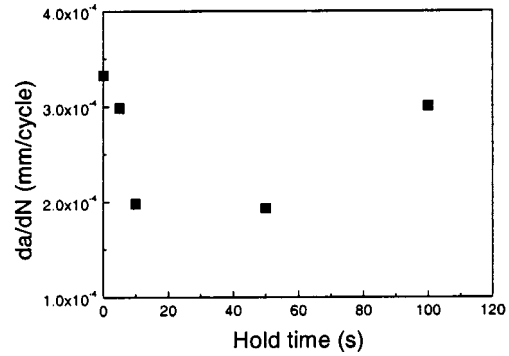

Figure 5. Crack growth rate as a function of hold time. At ΔK is 23MPa$\sqrt{m}$.

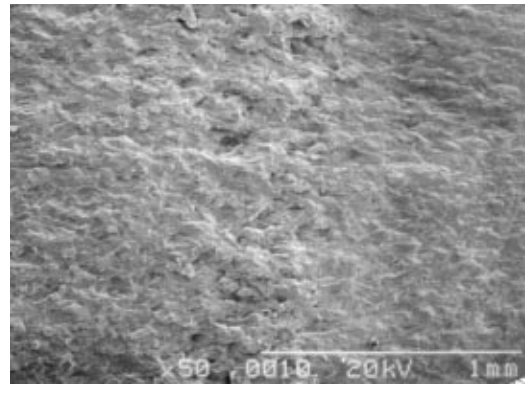

Figure 6. Fractured surface of fatigue crack growth test with 80 min. hold time applied at the maximum load in Figure 4.

causes blunting at the crack tip due to creep deformation and since resharpening time is required for crack to propagate again, the overall crack growth rate decreases.

Figure 5 shows the crack growth rates where ΔK is 23 MPa$\sqrt{m}$ for each hold time. This result is similar to the study of Adefris *et al*. (1996), with 1Cr-1Mo-0.25V steel. In trapezoidal waveform, the crack growth rate at the increasing and decreasing load parts, which is the crack growth rate of fatigue, decreases gradually with increasing hold time due to creep deformation. On the other hand, in the part where tensile hold time was applied, the crack growth rate increases as the tensile hold time increases due to creep. As a result, in relatively short tensile hold time, overall crack growth rate decreases due to blunting at the crack tip and cycle-dependent crack growth behavior is dominating. As the tensile hold time increases, crack growth rate by creep increases causing overall crack growth rate to increase and time-dependent crack growth behavior is dominating.

Figure 6 is the SEM photograph of a fracture surface of the fatigue test specimen with the applied tensile hold time of 80 min. at the maximum load during pure fatigue test. In the photograph, dimples caused by creep deformation were observed on the fracture surface, which indicates the occurrence of blunting at the crack tip that would lead to the decrease in crack growth rate.

3.2. Microstructure and Tensile Test of Each Aged Specimen

Table 3 shows the grain size and hardness of the aged specimens. The change in grain size against the aging time was negligible, however, a significant increase in hardness in the 1000 hr. and 2200 hr. aged specimens, which is believed to be the result of well dispersed carbides in the matrix and at the grain boundaries, was noted. Table 4 shows the tensile properties of the aged specimens.

At room temperature, both tensile and yield strengths of 1000 hr. aged specimen were the greatest, with the least ductility value. However, there was not much difference between 1000 hr. and 2200 hr. aged specimens. At 650°C, 2200 hr. aged specimen showed the greatest value in yield and tensile strength, however, again, there was not much difference between 1000 hr. and 2200 hr. aged specimens.

Figure 7 shows optical microstructures of each aged specimen. As the etchant, Glyceregia, etches precipitates preferentially, Figure 7a shows only the grain boundaries, revealing few precipitates formed at the grain boundaries. Figure 7b, which is the microstructure of 100 hr. aged specimen at 750°C, shows carbides at the grain boundary and a few carbides in the matrix. Figure 7c is the microstructure of 1000 hr. aged specimen at 750°C and shows coarsened carbides both in the matrix and at the grain boundary. In case of 2200 hr. aged specimen, Figure 7d, more coarsened carbides were found in the whole matrix and at the boundaries. Laves and σ phase precipitates were not found with the optical microscope.

Table 3. Grain size and hardness of aged specimens.

Aging Time (hr.)	0	100	1000	2200
Grain Size ASTM No.	6.9	6.8	6.9	6.8
Hardness Rockwell B	71	71	78	79

Table 4. Tensile properties of aged specimens.

	Aging Time (hr.)	0	100	1000	2200
Room Temp.	Y.S. (MPa)	229.8	225.3	310.1	293.6
	U.T.S. (Mpa)	590.9	569.1	612.7	590.7
	Elongation (%)	51.7	48.1	42.2	46.5
	R.A. (%)	77.6	66.2	50.4	48.7
650°C	Y.S. (MPa)	117.7	82.9	165.8	172.9
	U.T.S. (Mpa)	348.2	340.7	362.2	362.0
	Elongation (%)	29.0	24.4	37.5	28.9
	R.A. (%)	71.6	59.4	45.3	51.1

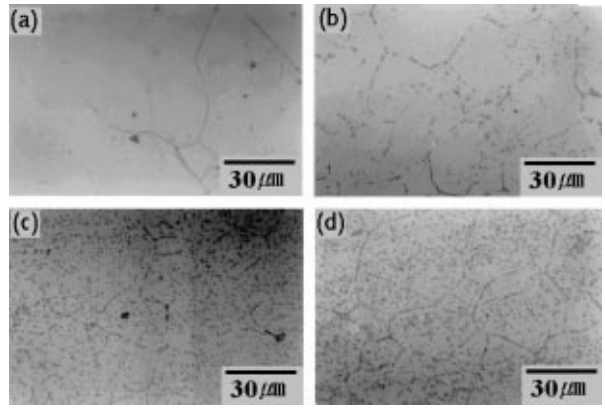

Figure 7. Microstructures of each aged specimen: (a) not aged; (b) 100 hr. at 750°C; (c) 1000 hr. at 750°C; (d) 2200 hr. at 750°C (etchant: Glyceregia).

3.3. Creep Rupture Tests of Each Aged Specimen

Figure 8 shows the creep elongation of the each aged specimen. Except the 250 MPa applied specimens, the creep elongation values increase significantly in 100 hr. aged specimens followed by decrease in 1000 hr. aged specimens and increase again in the 2200 hr. specimens. This tendency is believed to be the result of relatively easy glide of dislocations, where the solutionized carbon

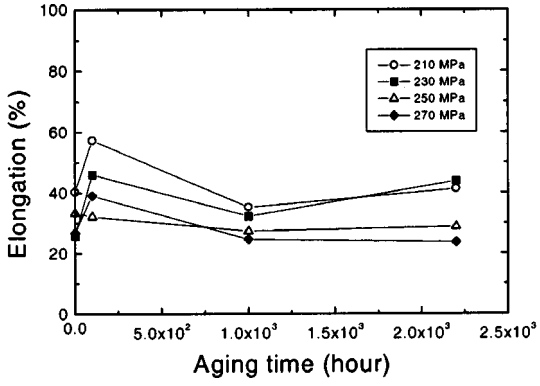

Figure 8. Effect of aging time on creep ductility.

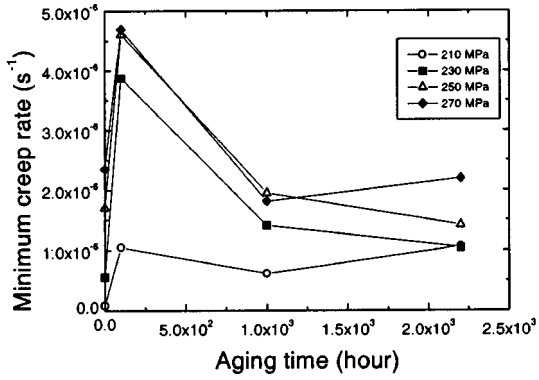

Figure 9. Effect of aging time on minimum creep rate.

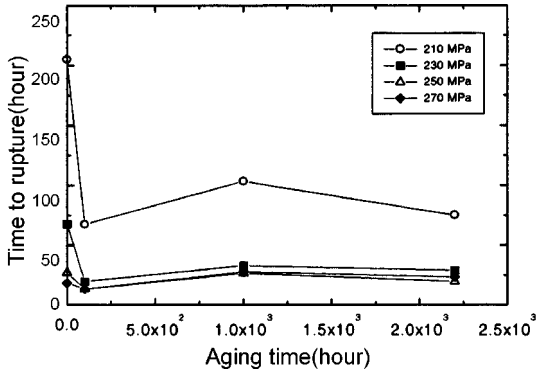

Figure 10. Effect of aging time on time to rupture.

content was low due to formation of carbide precipitates. The highest elongation values in each specimens were from the 100 hr. aged specimens and it is thought to be the result of the easier grain boundary sliding with the finer carbides than those of 1000 hr. and 2200 hr. aged specimens.

Figure 9 shows the minimum creep rate of each aged specimen. Under all applied stresses, the 100 hr. aged specimens showed the greatest rate and as the aging time gets longer, the rate decreased. This can be explained by the following assumptions that the fine grain boundary carbides of 100 hr. aged specimen made the grain boundary sliding easy, so the minimum creep rate increased. In case of 1000 hr. and 2200 hr. aged specimens, the coarsened grain boundary carbides made the grain boundary sliding more difficult, and the well dispersed carbides inside of the grains hindered the movement of dislocations as well.

Figure 10 shows the time to rupture for each aged specimen. The rupture life of 100 hr. aged specimen was the shortest under all applied stresses. In case of 1000 hr. aged specimen, the life increased a little, and in 2200 hr. aged specimen, the life decreased again. Although the elongation was the greatest in 100 hr. aged specimen, it had the shortest rupture life due to the fastest creep rate.

Fracture types were investigated with an optical microscope. Creep fracture types of all specimens were generally transgranular type fracture. In 1000 hr. aged specimen under the stress of 250 MPa, the cavity type microcracks were found at the interface of the carbide, which coarsened at grain boundary triple point. The microcracks grew transverse to the tensile direction, which is indicated by the elongation of the grains.

A triple point is known to be a favorable site to precipitate and as the carbide becomes the stress concentration point, it offers a crack initiation site. In 2200 hr. aged specimen under the initial stress of 270 MPa, cavitations formed at grain boundary carbide interfaces and they coalesced. The coalescent cavities became microcracks and propagated along the grain boundaries. Nevertheless, the transgranular type fracture dominated over the cavity type fracture in both cases. Figure 11 shows cavities in 1000 hr. and 2200 hr. aged specimens near the fracture surface. Under the constant temperature, in the power law creep regime, the stress dependence of the minimum creep rate of stainless steel is expressed by an equation of

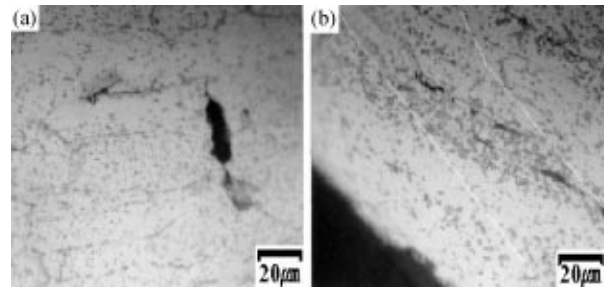

Figure 11. Microstructures of ruptured specimen: (a) 1000 hr. aged specimen (650°C/250 MPa); (b) 2200 hr. aged specimen (650°C/270 MPa).

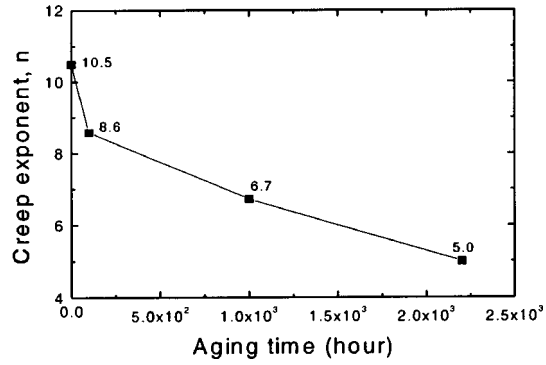

Figure 12. Effect of aging time on the creep exponent *n* at 650°C.

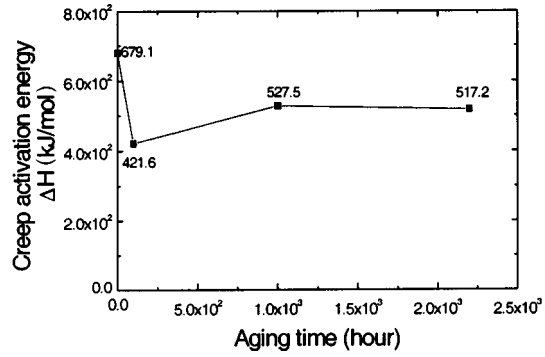

Figure 13. Effect of aging time on the creep activation energy ΔH at 230 MPa.

the form (Frost and Ashby, 1982).

$$\dot{\varepsilon}_m = A\sigma^n \tag{1}$$

where $\dot{\varepsilon}_m$ is the minimum creep rate, A is a constant, σ is an applied stress, and n is the creep exponent.

Figure 12 shows the measured value of n of each aged STS 316 specimen at 650°C. As the aging time increased, the n values decreased from 10.5 down to 5.0.

For the steady-state creep, the simplest assumption is that it is a singly activated process which can be expressed by an Arrhenius-type rate equation (Dieter, 1988).

$$\dot{\varepsilon}_m = Be^{-\Delta H/RT} \tag{2}$$

Where $\dot{\varepsilon}_m$ is the minimum creep rate, B is a constant, R is the universal gas constant, T is the absolute temperature, and ΔH is the activation energy for the rate-controlling process.

ΔH can be estimated by plotting ln $\dot{\varepsilon}_m$ vs. $1/T$, which can be obtained through a series of tests with small temperature intervals. Figure 13 shows the creep activation energy of each aged specimen. The measured value ranged from about 420 to 680 kJ/mol depending on the aging times. The change of minimum creep rate vs. aging time can be explained by the value of the creep activation energy, i.e. as the creep activation energy gets greater, the minimum creep rate becomes slower because the creep deformation is constricted. In contrast, as the creep activation energy becomes smaller, the minimum creep rate becomes faster.

4. CONCLUSIONS

In this study, STS 316L steel was tested for fatigue crack growth with various tensile hold times in trapezoidal waveform at 600°C and by using the prior aged STS 316 steel, creep rupture tests were conducted under various stress and temperature conditions. From the results, following conclusions were obtained.

(1) The STS 316L specimens showed a decrease in fatigue crack growth rate in relatively short tensile hold time region of up to 50 sec., compared with the pure fatigue, 0 sec. hold time applied case. But as the hold time increases to 100 sec., the crack growth rate began to increase again due to crack tip blunting.

(2) In STS 316 under initial stresses of 210 MPa-270 MPa, the 100 hr. aged specimens showed the shortest rupture life which was resulted from the highest minimum creep rate. And the 0 hr. aged specimens showed the longest rupture life, followed by 1000 hr. aged and 2200 hr. aged specimens.

(3) The value of the creep stress exponent, n, in $\dot{\varepsilon}_m = A\sigma^n$ decreased as the aging time increased. The measured n values for the 0 hr., 100 hr., 1000 hr., 2200 hr. aged specimens were 10.5, 8.6, 6.7 and 5.0 respectively.

(4) The creep activation energy, ?*H*, in $\dot{\varepsilon}_m = Be^{-\Delta H/RT}$, varied with the aging time. The activation energies for 0 hr., 100 hr., 1000 hr. and 2200 hr. aged specimens were calculated to be 679.1, 421.6, 527.5 and 517.2 kJ/mol respectively.

(5) The dominant creep rupture mechanism of all the aged specimens were the transgranular type fracture and in 1000 hr. and 2200 hr. aged specimens. The cavity type microcracks were found at the interface between coarse carbide and grain boundary.

ACKNOWLEDGEMENT–The authors are grateful for the support provided by a grant from the Korea Science & Engineering Foundation (KOSEF) and Safety and Structural Integrity Research Center at the Sungkyunkwan University.

REFERENCES

Adefris, N., Saxena, A. and McDowell, D. L. (1996). *Fatigue Fract. Engng. Mater. Struct.*, **19**(4), 401−411.

Annual Book of ASTM Standards (1995). Standard

Methods of Tension Testing of Metallic Materials, E8, ASTM, **3**(1), Philadelphia.

Annual Book of ASTM Standards (1995). Standard Practice for Conducting Creep, Creep-Rupture, and Stress-Rupture Tests of Metallic Materials, E139, ASTM, **3**(1), Philadelphia.

Annual Book of ASTM Standards (1995). Standard Practice for Elevated Temperature Tension Tests of Metallic Materials, E21, ASTM, **3**(1), Philadelphia.

Annual Book of ASTM Standards (1995). Standard Test Method for Measurement of Fatigue Crack Growth Rates, E647, ASTM, **3**(1), Philadelphia.

Biss, V. A. (1981). Metallographic study of type 304 stainless steel long term creep-rupture specimen, *Trans. Metall.*, A, **12A**, 1360.

Choe, B. H., Kang, S. H., Lee, J. H., Choi, J. H. and Hur, B. Y. (1997). Effect of the carbide behavior on creep properties of HK-40 heat resistant steel. *J. of the Korean Inst. of Met. & Mater.*, **35**(1), 23.

Dieter, G. E. (1988). *Mechanical Metallurgy*. 3rd ed. McGraw Hill, Printed in U.S.A., 450.

Frost, H. J. and Ashby, M. F. (1982). *Deformation-Mechanism Maps*, Pergamon Press, 11−12.

Hong, S. H. and Yu, J. (1989). Effect of prior austenite grain size on creep properties and on creep crack growth in 3.5Ni-Cr-Mo-V steel. *Scripta Metall*, **23**, 1057−1062.

Jata, K. V., Maxwell, D. and Nicholas, T. (1994). *J. Engng. Maters. and Tech.*, **116**, 45−53.

Kim, U.S. et al. (1996). Automobile Technical Handbook, *Trans. KSAE*, **4**, 8−12.

Kim, Y. S., Kim, S. E., Park, N. K. and Kim, H. M. (1990). Effect of heat treatment and HIPing on the creep properties of a nickel base superalloy IN 713LC, *J. of the Korean Inst. of Met. & Mater.*, **28**(10), 866.

Korea Standard (1991).Test pieces for tensile test for metallic materials, B0801.

Lee, J. H. (1997). *A Study on New Creep Fracture Parameter Considering Load Increasing Conditions.* Ph.D. Thesis, Sungkyunkwan University, Korea.

Nakanishi, T. (1977). A Study on the effect of helium environment and the grain size on the creep behaviour of hastelloy X alloy, *Journal of the Japan Institute of Metals*, **41**(3), 263.

Nam, S. W. and Hong, J. W. (1984). *J. Korea Society of Mechanical Engineering*, **24**(4), 225−261.

Parida, Basant K. and Theodore, Nicholas (1992). *Materials Science and Engineering*, **A153**, 493−498.

Shinya, N. (1982). Creep rupture property and micro-structure change in type 316 stainless steel, Tetsu-to-Hagane., **S1260**, 206.

Shinya, N. (1983). Creep rupture properties and creep fracture mechanism maps for type 304 stainless steel, *The Iron and Steel Institute of Japan*, **69**(14), 1668.

Shinya, N. (1985). Creep fracture mechanism maps on creep rupture test upto about 100000h for type 316 stainless steel, *The Iron and Steel Institute of Japan*, **71**(1), 114.